LIMNOLOGY and OCEANOGRAPHY: METHODS

ASLO

Limnol. Oceanogr.: Methods 22, 2024, 311–320

doi: 10.1002/lom3.10608

Interpreting biogeochemical processes through the relationship between total alkalinity and dissolved inorganic carbon: Theoretical basis and limitations

Hang Yin [1]*, **Lei Jin**,[2] **Xinping Hu** [1]

[1]Harte Research Institute for Gulf of Mexico Studies, Texas A&M University-Corpus Christi, Corpus Christi, Texas, USA
[2]Department of Mathematics and Statistics, Texas A&M University-Corpus Christi, Corpus Christi, Texas, USA

Abstract

The marine carbonate system is influenced by anthropogenic CO_2 uptake, biogeochemical processes, and physical changes that involve freshwater input and removal. Two frequently used parameters to quantify seawater carbonate system are total alkalinity (TA) and total dissolved inorganic carbon (DIC). To account for the physical changes, both TA and DIC are usually normalized to a reference salinity (i.e., nTA and nDIC), and then the relationship between nTA and nDIC is used to identify major biogeochemical processes that regulate the carbonate system, based on process-specific reaction stoichiometry. However, the theoretical basis of this interpretation has not been holistically examined. In this study, we validated this method under idealized conditions and discussed the associated assumptions and limitations. Furthermore, we applied this method to interpret field TA and DIC data from a lagoonal estuary in the northwestern Gulf of Mexico. Our results demonstrated that evaluating field data that encompass multiple stations and time periods could be problematic. In addition, various combinations of biogeochemical processes can lead to the same nTA–nDIC relationship, even though the relative importance of each individual process may vary significantly. Therefore, the stoichiometric relationship relying solely on TA and DIC data is not a definitive approach for uncovering dominant biogeochemical processes. Instead, measurements of process-specific parameters are necessary.

Total alkalinity (TA) and total dissolved inorganic carbon (DIC) are key parameters in marine carbonate chemistry and are often directly measured and used for speciation calculations (Orr et al. 2018). TA represents the number of moles of hydrogen ion equivalent to the excess of proton acceptors over proton donors with respect to the proton condition defined by the value $pK = 4.5$ in 1 kg of seawater (Dickson 1981). Wolf-Gladrow et al. (2007) expanded Dickson's definition of TA by using the electroneutrality of conservative species. TA is typically considered a semi-conservative parameter because its distribution in the open ocean is primarily influenced by physical processes (e.g., water mass mixing, precipitation, and evaporation) that control salinity (Millero et al. 1998). In addition, TA may also be influenced by biogeochemical reactions (Brewer and Goldman 1976; Goldman and Brewer 1980). DIC is the sum of dissolved inorganic carbon species in seawater, including aqueous CO_2, HCO_3^-, and CO_3^{2-}. Unlike TA, DIC is significantly influenced not only by air–sea exchange but also by processes that control TA, including biogeochemical processes such as respiration and photosynthesis, along with carbonate precipitation and dissolution (e.g., Hunt et al. 2022; Van Dam et al. 2021). Temperate and pressure changes affect pH and pCO_2, but both TA and DIC are not affected by those changes.

To account for conservative mixing of water masses with different salinities on TA and DIC, a normalization scheme against a fixed salinity (nTA and nDIC) (Chen and Millero 1979; Friis et al. 2003) is commonly employed to investigate the impacts of metabolic activities on seawater carbonate chemistry (e.g., Courtney et al. 2021) or to differentiate metabolic effect from anthropogenic CO_2 signals (Peng et al. 1998). Moreover, the slope of nTA–nDIC relationship is also widely used to infer major biogeochemical processes affecting carbonate chemistry in coastal environment (Hunt et al. 2022; Szymczycha et al. 2023; Xiong et al. 2023; Yin et al. 2023). This data interpretation method is based on the

*Correspondence: hang.yin@tamucc.edu

Author Contribution Statement: H.Y. conducted the theoretical derivation and data analysis in consultation with X.H. and L.J. H.Y. wrote the initial manuscript, and X.H. and L.J. provided input and feedback.

Additional Supporting Information may be found in the online version of this article.

premise that different biogeochemical processes affect TA and DIC differently (Table 1).

However, the theoretical basis and assumptions of this widely used method have not been holistically discussed. In this study, we examined the theoretical relationship between nTA and nDIC as well as $\Delta TA_i^*/\Delta DIC_i^*$ ratio under idealized conditions with defined boundary values (i.e., two endmember salinity, TA and DIC values), physical effects (i.e., mixing, precipitation, and evaporation), and reaction terms. Here, ΔTA_i^* and ΔDIC_i^* are defined as the differences between the linearly regressed values from TA–S and DIC–S relationships and the corresponding measurement values, and i denotes a random observation (Fig. 1A,B). Results showed that both the slope of nTA–nDIC relationship and $\Delta TA_i^*/\Delta DIC_i^*$ ratio would reflect the stoichiometry of biogeochemical reactions under these idealized conditions, but this approach has significant limitations when applied to field data.

Theoretical basis

Mixing-reaction model and normalization of TA and DIC

A two endmember conservative mixing model has been widely used to study TA and DIC behaviors along a salinity gradient (e.g., Cabral et al. 2021; Cai et al. 2003; Friis et al. 2003; Hunt et al. 2022; Liu et al. 2021; Yang and Byrne 2023). In this model, there are n observations, with each observation comprising measurements for salinity, TA, and DIC. Both the observation of TA (TA_{obs}) and observation of DIC (DIC_{obs}) can be expressed by a conservative mixing term and a biogeochemical reaction term. Air–sea exchange, which affects DIC only, is included in the reaction term throughout this paper, and to enhance clarity, we employ a notation involving parameters such as TA and DIC, each subscripted with a positive integer i or j to represent the i^{th} or j^{th} observation of the parameter along the theoretical salinity gradient. The model for TA_{obs} is:

$$TA_{obs,i} = k_{TA}S_i + eTA_0 + \Delta TA_i \quad (1)$$

where k_{TA} is the slope of TA along with S due to conservative mixing, derived from the mixing line based on two known endmembers; S_i is the salinity of the i^{th} observation (assuming not affected by biogeochemical reactions); e is the evaporation factor, which accounts for the net evaporation effect (Supporting Information Appendix A, *see* also in Yin et al. (2023)); TA_0 represents the river endmember ($S = 0$) TA; and ΔTA_i represents the apparent change (i.e., evaporation effect is included) in TA of the i^{th} observation due to biogeochemical reactions (i.e., reaction term). Therefore, $k_{TA}S_i + eTA_0$ represents the conservative mixing term of the i^{th} TA observation.

Similarly, the model for DIC_{obs} is:

$$DIC_{obs,i} = k_{DIC}S_i + eDIC_0 + \Delta DIC_i \quad (2)$$

where k_{DIC} is the slope of DIC along with S due to conservative mixing, derived from the mixing line based on two known endmembers; DIC_0 represents the river endmember ($S = 0$) DIC; and ΔDIC_i represents the apparent change in DIC of the i^{th} observation due to reactions. Therefore, $k_{DIC}S_i + eDIC_0$ represents the conservative mixing term of the i^{th} DIC observation.

Assuming the changes in TA and DIC due to biogeochemical reactions (i.e., ΔTA_i and ΔDIC_i) in each observation follow a constant ratio β, which is determined by the processes in Table 1:

Table 1. Representative biogeochemical and physical processes that affect carbonate chemistry and their corresponding stoichiometric alterations to TA and DIC. Note that this list is not exhaustive. Table compiled after Hunt et al. (2022) and Middelburg et al. (2020).

Process	Formula	ΔTA : ΔDIC
Primary production (nitrate)	$106CO_2 + 16HNO_3 + H_3PO_4 + 122H_2O \rightarrow (CH_2O)_{106}(NH_3)_{16}(H_3PO_4) + 138O_2$	17 : −106
Primary production (ammonium)	$106CO_2 + 16NH_3 + H_3PO_4 + 106H_2O \rightarrow (CH_2O)_{106}(NH_3)_{16}(H_3PO_4) + 106O_2$	−15 : −106
Aerobic remineralization (ammonium)	$(CH_2O)_{106}(NH_3)_{16}(H_3PO_4) + 106O_2 \rightarrow 106CO_2 + 16NH_3 + H_3PO_4 + 106H_2O$	15 : 106
Aerobic remineralization (nitrate)	$(CH_2O)_{106}(NH_3)_{16}(H_3PO_4) + 138O_2 \rightarrow 106CO_2 + 16HNO_3 + H_3PO_4 + 122H_2O$	−17 : 106
Nitrification	$NH_4^+ + 2O_2 \rightarrow HNO_3 + H_2O + H^+$	−2 : 0
Denitrification	$5(CH_2O)_{106}(NH_3)_{16}(H_3PO_4) + 424HNO_3 \rightarrow 530CO_2 + 212\ N_2 + 742H_2O + 5H_3PO_4 + 80NH_3$	499 : 530
Sulfate reduction	$(CH_2O)_{106}(NH_3)_{16}(H_3PO_4) + 53SO_4^{2-} + 53H^+ \rightarrow 106CO_2 + 53HS^- + 106H_2O + H_3PO_4 + 16NH_3$	121 : 106
Sulfide oxidation	$H_2S + 2O_2 \rightarrow SO_4^{2-} + 2H^+$	−2 : 0
Carbonate dissolution/precipitation	$CaCO_3 \leftrightarrow Ca^{2+} + CO_3^{2-}$	2 : 1 or −2 : −1
Iron oxide reduction	$(CH_2O)_{106}(NH_3)_{16}(H_3PO_4) + 424Fe(OH)_3 + 848H^+ \rightarrow 106CO_2 + 424Fe^{2+} + 1166H_2O + H_3PO_4 + 16NH_3$	863 : 106
CO_2 exchange	$CO_2(g) \leftrightarrow CO_2(aq)$	0 : ±1

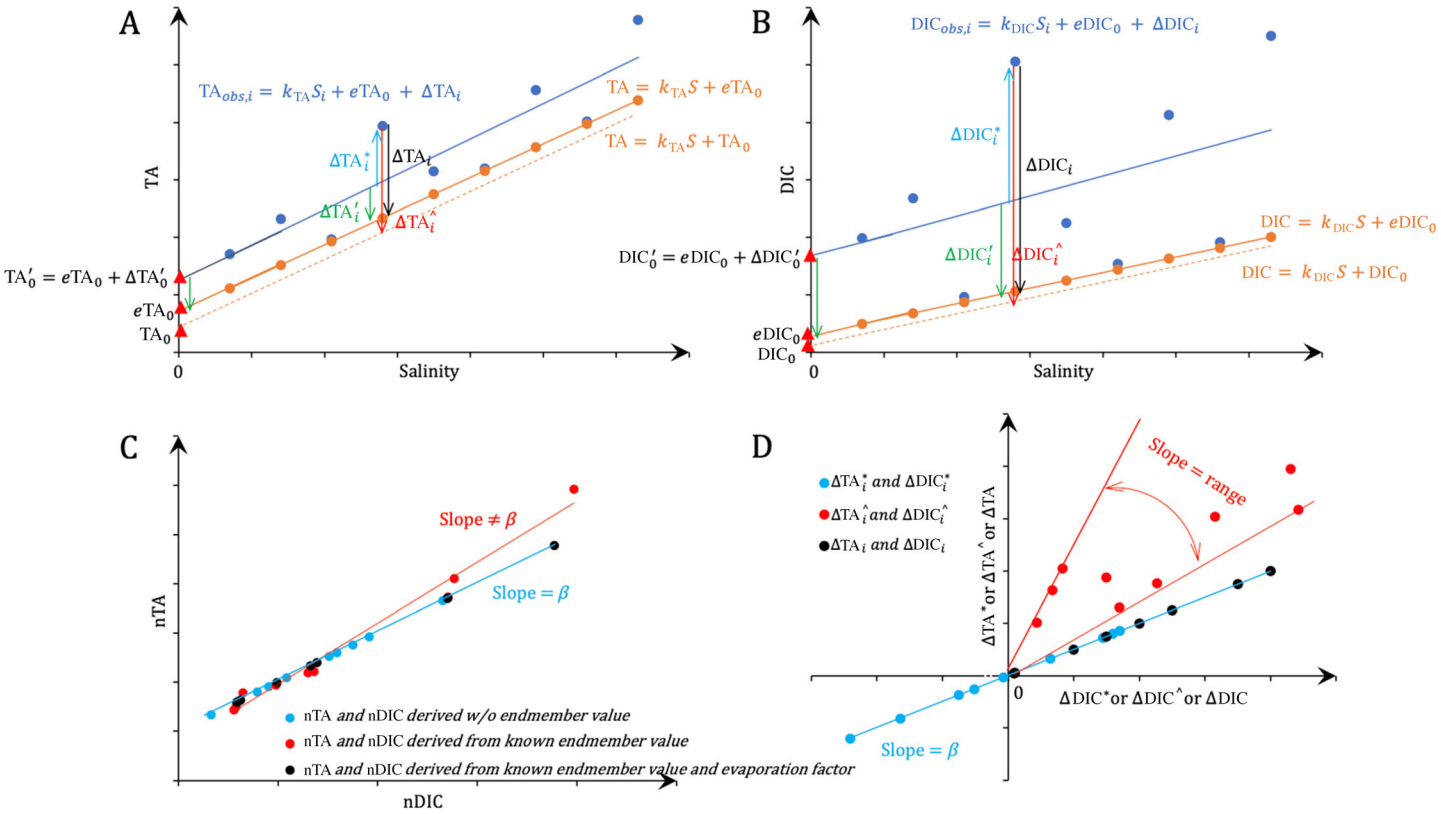

Fig. 1. Schematic plots of TA or DIC–salinity relationship (**A**,**B**), nTA–nDIC relationship (**C**), and changes of TA–changes of DIC relationship (**D**). In (**A**) and **(B)**, blue dots represent observation values. Blue lines represent linear regressions of observation values. Solid orange lines represent conservative mixing after evaporation correction. Dashed orange lines represent conservative mixing without evaporation correction. Black vertical arrows represent differences between observation values and conservative mixing lines after evaporation correction. Red vertical arrows represent differences between observation values and conservative mixing lines without evaporation correction. Blue vertical arrows represent differences between linear regression lines and observation values. Green vertical arrows represent differences between linear regression lines and conservative mixing lines after evaporation correction. Red triangles represent *y*-axis intercepts of three relationships. In (**C**), solid lines represent linear regressions of nTA and nDIC, which are calculated by different methods. Note that blue and black dots follow the same linear relationship. In (**D**), color codings of dots represent changes of TA and DIC calculated by different methods.

$$\beta = \frac{\Delta TA_i}{\Delta DIC_i} \tag{3}$$

ΔTA_i^* and ΔDIC_i^* should follow (Fig. 1A,B; Supporting Information Appendix B):

$$\beta = \frac{\Delta TA_i^*}{\Delta DIC_i^*} \tag{4}$$

At the same time, the differences between the predicted values of the least squares regression and the conservative mixing values after evaporation correction for TA and DIC ($\Delta TA_i'$ and $\Delta DIC_i'$, respectively; Fig. 1A,B) should also follow (Supporting Information Appendix B):

$$\beta = \frac{\Delta TA_i'}{\Delta DIC_i'} \tag{5}$$

Equations (1) and (2) incorporate the mixing term, the evaporation term, and the reaction term. The sequence of these processes does not alter the explicit expressions of TA_{obs} and DIC_{obs}, as shown in Eqs. 1 and 2, and the hypothesized relationship between ΔTA_i and ΔDIC_i (i.e., Eq. 3) (Supporting Information Appendix C). When considering a river endmember with nonzero salinity, a pseudo freshwater endmember can be extrapolated for use in Eqs. 1 and 2 (Supporting Information Appendix D). Under this special condition, TA_0 and DIC_0 serve solely as formal representations of the zero salinity endmembers for TA and DIC. These treatments do not change the explicit expressions of TA_{obs}, DIC_{obs}, nor the $\Delta TA_i/\Delta DIC_i$ ratio (Supporting Information Appendix D).

Based on Eqs. 1 and 2, observations for TA, DIC, and salinity are explicitly listed in Box 1.

To correct for the salinity differences in observations, nTA and nDIC can be calculated following Friis et al. (2003):

Box 1. Observations for S, TA, and DIC.

S	TA_{obs}	DIC_{obs}
S_1	$k_{TA}S_1 + eTA_0 + \Delta TA_1$	$k_{DIC}S_1 + eDIC_0 + \Delta DIC_1$
S_2	$k_{TA}S_2 + eTA_0 + \Delta TA_2$	$k_{DIC}S_2 + eDIC_0 + \Delta DIC_2$
⋮	⋮	⋮
S_n	$k_{TA}S_n + eTA_0 + \Delta TA_n$	$k_{DIC}S_n + eDIC_0 + \Delta DIC_n$

$$nTA = \left(\frac{TA_{obs} - TA'_0}{S_{obs}} \times S_{ref}\right) + TA'_0 \quad (6)$$

$$nDIC = \left(\frac{DIC_{obs} - DIC'_0}{S_{obs}} \times S_{ref}\right) + DIC'_0 \quad (7)$$

where S_{ref} is the reference salinity; TA'_0 and DIC'_0 are the zero-salinity TA and DIC, respectively. In practice, TA'_0 and DIC'_0 are determined from the corresponding intercept terms of the linear regressions of TA_{obs} and DIC_{obs} against salinity. Apparently, TA'_0 and DIC'_0 also follow (Fig. 1):

$$TA'_0 = eTA_0 + \Delta TA'_0 \quad (8)$$

$$DIC'_0 = eDIC_0 + \Delta DIC'_0 \quad (9)$$

where again $e, TA_0, DIC_0, \Delta TA'_0, \text{and} \Delta DIC'_0$ have the same definitions previously provided in Eqs. 1, 2, and 5.

The nTA–nDIC relationship and $\Delta TA^*_i/\Delta DIC^*_i$ ratio derived without endmember value

Based on Box 1 and Eqs. 6–9, nTA and nDIC can be expressed as follows (Box 2):

For any two given i^{th} and j^{th} observations of nTA (i.e., nTA_i and nTA_j) and nDIC (i.e., $nDIC_i$ and $nDIC_j$), the slope of nTA–nDIC relationship (i.e., $\Delta nTA/\Delta nDIC$) can be derived as follows:

Box 2. Calculated nTA and nDIC.

S	nTA	nDIC
S_{ref}	$\frac{k_{TA}S_1+\Delta TA_1-\Delta TA'_0}{S_1}S_{ref}+TA'_0$	$\frac{k_{DIC}S_1+\Delta DIC_1-\Delta DIC'_0}{S_1}S_{ref}+DIC'_0$
S_{ref}	$\frac{k_{TA}S_2+\Delta TA_2-\Delta TA'_0}{S_2}S_{ref}+TA'_0$	$\frac{k_{DIC}S_2+\Delta DIC_2-\Delta DIC'_0}{S_2}S_{ref}+DIC'_0$
⋮	⋮	⋮
S_{ref}	$\frac{k_{TA}S_n+\Delta TA_n-\Delta TA'_0}{S_n}S_{ref}+TA'_0$	$\frac{k_{DIC}S_n+\Delta DIC_n-\Delta DIC'_0}{S_n}S_{ref}+DIC'_0$

$$\frac{\Delta nTA}{\Delta nDIC} = \frac{nTA_i - nTA_j}{nDIC_i - nDIC_j} = \frac{S_{ref}\left(k_{TA} + \frac{\Delta TA_i - \Delta TA'_0}{S_i}\right) + TA'_0 - S_{ref}\left(k_{TA} + \frac{\Delta TA_j - \Delta TA'_0}{S_j}\right) - TA'_0}{S_{ref}\left(k_{DIC} + \frac{\Delta DIC_i - \Delta DIC'_0}{S_i}\right) + DIC'_0 - S_{ref}\left(k_{DIC} + \frac{\Delta DIC_j - \Delta DIC'_0}{S_j}\right) - DIC'_0} = \frac{\frac{\Delta TA_i - \Delta TA'_0}{S_i} - \frac{\Delta TA_j - \Delta TA'_0}{S_j}}{\frac{\Delta DIC_i - \Delta DIC'_0}{S_i} - \frac{\Delta DIC_j - \Delta DIC'_0}{S_j}} \quad (10)$$

According to Eqs. 3 and 5:

$$\frac{\frac{\Delta TA_i - \Delta TA'_0}{S_i}}{\frac{\Delta DIC_i - \Delta DIC'_0}{S_i}} = \frac{\beta\Delta DIC_i - \beta\Delta DIC'_0}{\Delta DIC_i - \Delta DIC'_0} = \beta \quad (11)$$

$$\frac{\frac{\Delta TA_j - \Delta TA'_0}{S_j}}{\frac{\Delta DIC_j - \Delta DIC'_0}{S_j}} = \frac{\beta\Delta DIC_j - \beta\Delta DIC'_0}{\Delta DIC_j - \Delta DIC'_0} = \beta \quad (12)$$

According to Eqs. 11 and 12, Eq. (10) can be rearranged as follows:

$$\frac{\Delta nTA}{\Delta nDIC} = \frac{\beta\frac{\Delta DIC_i - \Delta DIC'_0}{S_i} - \beta\frac{\Delta DIC_j - \Delta DIC'_0}{S_j}}{\frac{\Delta DIC_i - \Delta DIC'_0}{S_i} - \frac{\Delta DIC_j - \Delta DIC'_0}{S_j}} = \beta \quad (13)$$

The intercept of nTA–nDIC relationship can be calculated from observations i or j as follows:

$$nTA_i - \beta nDIC_i = \frac{k_{TA}S_i + \Delta TA_i - \Delta TA'_0}{S_i}S_{ref} + TA'_0 - \beta\left(\frac{k_{DIC}S_i + \Delta DIC_i - \Delta DIC'_0}{S_i}S_{ref} + DIC'_0\right) \quad (14)$$

Furthermore, via Eqs. 3, 5, 8, and 9, Eq. 14 can be rearranged as follows:

$$nTA_i - \beta nDIC_i = S_{ref}(k_{TA} - \beta k_{DIC}) + eTA_0 - \beta eDIC_0 \quad (15)$$

Therefore, nTA and nDIC for all observations follow a linear relationship with a slope of β and an intercept of $S_{ref}(k_{TA} - \beta k_{DIC}) + eTA_0 - e\beta DIC_0$, and the linear relationship quantitively reflects the reaction stoichiometry, the reference salinity, the TA–S and DIC–S river–ocean conservative mixing relationships, and the evaporation factor. Similarly, $\Delta TA^*_i/\Delta DIC^*_i = \beta$ (Eq. 4) also reflects the reaction stoichiometry (Fig. 1C,D).

The slope of nTA–nDIC relationship and $\Delta TA^{\wedge}_i/\Delta DIC^{\wedge}_i$ ratio derived from known endmember value

If river endmember TA_0 and DIC_0 are directly measured and used for the nTA and nDIC calculations (i.e., assume

$TA'_0 = TA_0$ and $DIC'_0 = DIC_0$), nTA and nDIC can be calculated according to Box 1 and Eqs. 6 and 7 as follows (Box 3):

For any two given i^{th} and j^{th} observations of nTA (i.e., nTA_i and nTA_j) and nDIC (i.e., $nDIC_i$ and $nDIC_j$), the slope of nTA–nDIC relationship can be calculated as follows:

$$\begin{aligned}\frac{\Delta nTA}{\Delta nDIC} &= \frac{S_{ref}\left(k_{TA}+\frac{(e-1)TA_0+\Delta TA_i}{S_i}\right)+TA_0-S_{ref}\left(k_{TA}+\frac{(e-1)TA_0+\Delta TA_j}{S_j}\right)-TA_0}{S_{ref}\left(k_{DIC}+\frac{(e-1)DIC_0+\Delta DIC_i}{S_i}\right)+DIC_0-S_{ref}\left(k_{DIC}+\frac{(e-1)DIC_0+\Delta DIC_j}{S_j}\right)-DIC_0}\\ &= \frac{\frac{(e-1)TA_0+\Delta TA_i}{S_i}-\frac{(e-1)TA_0+\Delta TA_j}{S_j}}{\frac{(e-1)DIC_0+\Delta DIC_i}{S_i}-\frac{(e-1)DIC_0+\Delta DIC_j}{S_j}}\\ &= \frac{(e-1)\left(\frac{TA_0}{S_i}-\frac{TA_0}{S_j}\right)+\left(\frac{\Delta TA_i}{S_i}-\frac{\Delta TA_j}{S_j}\right)}{(e-1)\left(\frac{DIC_0}{S_i}-\frac{DIC_0}{S_j}\right)+\left(\frac{\Delta DIC_i}{S_i}-\frac{\Delta DIC_j}{S_j}\right)}\end{aligned} \quad (16)$$

Therefore, when including the river endmember value without evaporation correction, the nTA–nDIC relationship does not reflect the stoichiometry of biogeochemical reactions (Fig. 1C).

For the i^{th} observation, let $\Delta\hat{TA}_i$ and $\Delta\hat{DIC}_i$ be the differences between the TA or DIC observation values and the corresponding values based on endmember conservative mixing without evaporation correction (Fig. 1A,B). Similarly, $\Delta\hat{TA}_i/\Delta\hat{DIC}_i$ also does not reflect the reaction stoichiometry (Fig. 1D):

$$\begin{aligned}\frac{\Delta\hat{TA}_i}{\Delta\hat{DIC}_i} &= \frac{k_{TA}S_i+eTA_0+\Delta TA_i-k_{TA}S_i-TA_0}{k_{DIC}S_i+eDIC_0+\Delta DIC_i-k_{DIC}S_i-DIC_0}\\ &= \frac{(e-1)TA_0+\Delta TA_i}{(e-1)DIC_0+\Delta DIC_i}\end{aligned} \quad (17)$$

The slope of nTA–nDIC relationship and $\Delta TA_i/\Delta DIC_i$ ratio derived from known endmember value and evaporation factor

If river endmember TA_0, DIC_0, and evaporation factor (i.e., eTA_0, $eDIC_0$) are known and used for the nTA and nDIC calculations (i.e., assume $TA'_0 = eTA_0$ and $DIC'_0 = eDIC_0$), nTA and nDIC can be calculated according to Box 1 and Eqs. 6 and 7 as follows (Box 4):

For any two given i^{th} and j^{th} observations of nTA (i.e., nTA_i and nTA_j) and nDIC (i.e., $nDIC_i$ and $nDIC_j$), the slope of nTA–nDIC relationship can be calculated as follows:

$$\begin{aligned}\frac{\Delta nTA}{\Delta nDIC} &= \frac{\frac{k_{TA}S_i+\Delta TA_i}{S_i}S_{ref}+eTA_0-\frac{k_{TA}S_j+\Delta TA_j}{S_j}S_{ref}-eTA_0}{\frac{k_{DIC}S_i+\Delta DIC_i}{S_i}S_{ref}+eDIC_0-\frac{k_{DIC}S_j+\Delta DIC_j}{S_j}S_{ref}-eDIC_0}\\ &= \frac{\frac{\Delta TA_i}{S_i}-\frac{\Delta TA_j}{S_j}}{\frac{\Delta DIC_i}{S_i}-\frac{\Delta DIC_j}{S_j}}\end{aligned} \quad (18)$$

According to Eq. 3, Eq. 18 can be arranged as follows:

$$\frac{\Delta nTA}{\Delta nDIC} = \frac{\beta\frac{\Delta DIC_i}{S_i}-\beta\frac{\Delta DIC_j}{S_j}}{\frac{\Delta DIC_i}{S_i}-\frac{\Delta DIC_j}{S_j}} = \beta \quad (19)$$

Box 3. Calculated nTA and nDIC.

S	nTA	nDIC
S_{ref}	$\frac{k_{TA}S_1+(e-1)TA_0+\Delta TA_1}{S_1}S_{ref}+TA_0$	$\frac{k_{DIC}S_1+(e-1)DIC_0+\Delta DIC_1}{S_1}S_{ref}+DIC_0$
S_{ref}	$\frac{k_{TA}S_2+(e-1)TA_0+\Delta TA_2}{S_2}S_{ref}+TA_0$	$\frac{k_{DIC}S_2+(e-1)DIC_0+\Delta DIC_2}{S_2}S_{ref}+DIC_0$
⋮	⋮	⋮
S_{ref}	$\frac{k_{TA}S_n+(e-1)TA_0+\Delta TA_n}{S_n}S_{ref}+TA_0$	$\frac{k_{DIC}S_n+(e-1)DIC_0+\Delta DIC_n}{S_n}S_{ref}+DIC_0$

Box 4. Calculated nTA and nDIC.

S	nTA	nDIC
S_{ref}	$\frac{k_{TA}S_1+\Delta TA_1}{S_1}S_{ref}+eTA_0$	$\frac{k_{DIC}S_1+\Delta DIC_1}{S_1}S_{ref}+eDIC_0$
S_{ref}	$\frac{k_{TA}S_2+\Delta TA_2}{S_2}S_{ref}+eTA_0$	$\frac{k_{DIC}S_2+\Delta DIC_2}{S_2}S_{ref}+eDIC_0$
⋮	⋮	⋮
S_{ref}	$\frac{k_{TA}S_n+\Delta TA_n}{S_n}S_{ref}+eTA_0$	$\frac{k_{DIC}S_n+\Delta DIC_n}{S_n}S_{ref}+eDIC_0$

The intercept of nTA–nDIC relationship can be calculated from observations i or j as follows:

$$\begin{aligned} nTA_i - \beta nDIC_i &= \frac{k_{TA}S_i + \Delta TA_i}{S_i} S_{ref} + eTA_0 \\ &\quad - \beta\left(\frac{k_{DIC}S_i + \Delta DIC_i}{S_i} S_{ref} + eDIC_0\right) \\ &= S_{ref}(k_{TA} - \beta k_{DIC}) + eTA_0 - \beta eDIC_0 \end{aligned} \quad (20)$$

Therefore, nTA and nDIC for all observations follow a linear relationship with a slope of β and an intercept of $S_{ref}(k_{TA} - \beta k_{DIC}) + \alpha TA_0 - \alpha\beta DIC_0$ (Fig. 1C). By assumption (Eq. 3), the $\Delta TA_i/\Delta DIC_i$ ratio also reflects the reaction stoichiometry (Fig. 1D).

Will biogeochemical reaction affect the nTA–nDIC relationship, $\Delta TA_i^{\wedge}/\Delta DIC_i^{\wedge}$, and $\Delta TA_i^{*}/\Delta DIC_i^{*}$ by the stoichiometry?

Assuming that biogeochemical reactions affect TA and DIC through a constant ratio (β), $k_{TA}, k_{DIC}, TA_0, DIC_0$, and e remain constant for all the observations, the nTA–nDIC relationships are derived accordingly in three considerations: without endmember value; with only endmember value; and with endmember value and evaporation factor (Fig. 1C; Table 2). The slope of the nTA–nDIC relationship would not be β if nTA and nDIC are calculated using freshwater endmember values directly (i.e., $TA_0' = TA_0$ and $DIC_0' = DIC_0$) (Eq. 16). In the other two scenarios, the derived linear nTA–nDIC relationship has a slope of β and an intercept of $S_{ref}(k_{TA} - \beta k_{DIC}) + eTA_0 - e\beta DIC_0$ (Fig. 1C; Table 2). In the meantime, $\Delta TA_i^{*}/\Delta DIC_i^{*}$ equals β, while $\Delta TA_i^{\wedge}/\Delta DIC_i^{\wedge}$ does not (Fig. 1D; Table 2). Thus, we recommend using $\Delta TA_i^{*}/\Delta DIC_i^{*}$ or nTA–nDIC derived without endmember value for data interpretation due to the irrelevance to the evaporation factor, which is usually difficult to quantify, and the following discussion is based on this method. However, the values of the endmembers and the evaporation factor are critical for understanding the actual magnitude of change in TA or DIC due to biogeochemical processes.

In natural environments, a more realistic scenario involves the mixing of multiple endmembers, such as various rivers, hydrothermal vents, groundwater discharges, and different water masses. The theoretical basis derivations focused only on a mixing scenario with two endmembers, and the method described above does not apply to scenarios where more than two endmembers are involved. For instance, the normalization method, as outlined in Eqs. 6 and 7, cannot be employed in such cases. In addition, the effect of biogeochemical processes from both the water column and sediment can exhibit spatial and temporal variations and thus may not be constant for all the observations, invalidating the assumptions underlying this method. For example, in the Chesapeake Bay, there is a spatial separation of carbonate mineral formation upstream and carbonate dissolution downstream, which functions as a pH buffer (Su et al. 2020). In addition, the relative contribution from aerobic respiration was also different in the same region (Su et al. 2020). In another case, sulfide oxidation was observed in semi-arid estuaries in the northwestern Gulf of Mexico during prolonged periods of extreme drought, but this sulfate enrichment signal was not observed during non-drought years (Dias et al. 2022; Yin et al. 2023). Incorporating observations from different spatial or temporal ranges, which undergo a number of processes with different β values, can lead to decreased linearity in the nTA–nDIC relationship as well as changes in $\Delta TA_i^{*}/\Delta DIC_i^{*}$ ratio. Furthermore, the spatial and temporal variations in $k_{TA}, k_{DIC}, TA_0, DIC_0$, and e can also affect the linearity of the nTA–nDIC relationship and $\Delta TA_i^{*}/\Delta DIC_i^{*}$ values. The method itself is overly simplistic in some of the cases, and we therefore suggest thoroughly evaluating the assumptions of the method when applying it to interpret field data.

It is worthwhile to note that the regression-based TA_0' and DIC_0' can vary significantly from the directly measured freshwater endmember TA and DIC values (i.e., TA_0 and DIC_0). Only under certain conditions, such as a two endmember mixing scenario with a low salinity freshwater endmember (Supporting Information Appendix D), nearly balanced freshwater evaporation and precipitation (i.e., $e \approx 1$) and negligible $\Delta TA_0'$ and $\Delta DIC_0'$ (i.e., reaction terms being minor or fast river–ocean mixing), can the respective intercepts accurately reflect the freshwater endmember TA and DIC values. In such cases, variations in nTA and nDIC may be small (Box 2), but the slope of the nTA–nDIC relationship can still be significant (Eq. 13). However, these assumptions may not always

Table 2. Summary of the theoretical relationship of nTA–nDIC, and ratios of $\Delta TA_i^{*}/\Delta DIC_i^{*}$, $\Delta TA_i^{\wedge}/\Delta DIC_i^{\wedge}$, and $\Delta TA_i/\Delta DIC_i$.

	nTA–nDIC		$\frac{\Delta TA_i^{*}}{\Delta DIC_i^{*}}$, $\frac{\Delta TA_i^{\wedge}}{\Delta DIC_i^{*}}$, or $\frac{\Delta TA_i}{\Delta DIC_i}$
Parameter requirement	**Slope**	**Intercept**	**Ratio**
No endmember value required	β	$S_{ref}(k_{TA} - \beta k_{DIC}) + eTA_0 - \beta eDIC_0$	$\frac{\Delta TA_i^{*}}{\Delta DIC_i^{*}} = \beta$
Endmember value only	$\neq \beta$	Variable	$\frac{\Delta TA_i^{\wedge}}{\Delta DIC_i^{*}} \neq \beta$
Endmember value and evaporation factor	β	$S_{ref}(k_{TA} - \beta k_{DIC}) + eTA_0 - \beta eDIC_0$	$\frac{\Delta TA_i}{\Delta DIC_i} = \beta$

hold in some estuaries (e.g., estuaries located in the northwestern Gulf of Mexico), where both net evaporation and biogeochemical influences cannot be ignored. Thus, it is not proper to apply this method to extrapolate for the freshwater endmember values in such cases.

Field data examination

Data collection

The Mission-Aransas Estuary (MAE) is a unique ecosystem located in the northwestern Gulf of Mexico coast. It is a semi-arid estuarine system that receives freshwater from the Mission River and the Aransas River. Both rivers experience low base flows interspersed with periodic high flows during storms (McCutcheon et al. 2021). Freshwater inflow plays a crucial role in maintaining the balance of the estuarine ecosystem.

Water samples were collected from the MAE every 2 weeks during the summer months and monthly during the winter months between May and December in 2014, encompassing a drought period. A total of six stations were visited during each cruise (Aransas Bay [27.9797°N, 97.0286°W]; Copano East [28.1322°N, 97.0344°W]; Copano West [28.0839°N, 97.2008°W]; Little Bay [28.0367°N, 97.0325°W]; Mesquite Bay [28.1383°N, 96.8283°W]; Ship Channel [27.8381°N, 97.0503°W]). At each station, both surface (0.1 m) and bottom (up to 7 m) water samples were collected following the standard protocol for ocean carbonate chemistry studies (Dickson et al. 2007).

DIC was analyzed using infrared detection on an AS-C3 DIC analyzer (Apollo SciTech Inc.). TA was measured at 22°C on an AS-ALK2 alkalinity titrator (Apollo SciTech Inc.) following the principle of Gran titration (Gran 1952) for endpoint determination. Salinity was measured using a benchtop salinometer. To ensure the accuracy of DIC, TA, and salinity measurements, Certified Reference Material from Scripps Institution of Oceanography at University of California, San Diego was used.

What information can be inferred from the field data TA and DIC stoichiometry?

Data from all five stations were analyzed collectively (Fig. 2A,C,E,G). The plots of TA_{obs} and DIC_{obs} vs. salinity from the MAE ($R^2 = 0.23$ and 0.09, respectively) indicated that the reaction terms, ΔTA_i and ΔDIC_i, varied at each observation during the sampling period (Fig. 2A,C). Based on the assumption of constant $k_{TA}, k_{DIC}, TA_0, DIC_0, \beta,$ and e, from both the slope of nTA–nDIC relationship and individual $\Delta TA_i^*/\Delta DIC_i^*$ ratio (Fig. 2E,G), the reactions affected TA and DIC by $\beta = 1.1$. Based on the β value alone, the major processes that led to variations in TA and DIC would be sulfate reduction and denitrification, which would theoretically result in ratios of $\Delta TA_i/\Delta DIC_i$ 1.14 and 0.94, respectively (Table 1). However, this interpretation is not likely to be true because the studied area is typically nitrogen limited (Mooney and McClelland 2012). Instead, sulfide oxidation and carbonate dissolution/precipitation with different $\Delta TA_i/\Delta DIC_i$ likely occurred during the study period (Dias et al. 2022; Yin et al. 2023).

The high linearity of the nTA–nDIC relationship ($R^2 = 0.93$) and the consistency in individual $\Delta TA_i^*/\Delta DIC_i^*$ ratios (Fig. 2E,G) imply $k_{TA}, k_{DIC}, TA_0, DIC_0, \beta,$ and e did not change significantly throughout the observation period and across locations. However, when a specific subset (i.e., Copano West station) of the dataset was analyzed (Fig. 2B,D,F,H), a different $\Delta TA_i/\Delta DIC_i$ was obtained (Fig. 2F,H). Both nTA–nDIC relationship and $\Delta TA_i^*/\Delta DIC_i^*$ ratio suggested a β value ranging from 1.4 to 1.9, which is higher than the calculated value using the entire dataset. To adequately meet the conditions of the assumptions, it is recommended to use a dataset that is more localized and spans a shorter period of time. However, in reality, establishing clear boundaries for the selection of sample locations and timeframes could be challenging.

Although some reactions have similar stoichiometry (e.g., sulfate reduction and denitrification), β value reflects the combined influence from a series of x reactions, where x is the total number of reactions considered. β can also be derived as follows:

$$\frac{\Delta TA_i}{\Delta DIC_i} = \frac{\Delta TA(1)\times\gamma(1) + \Delta TA(2)\times\gamma(2) + \cdots + \Delta TA(x)\times\gamma(x)}{\Delta DIC(1)\times\gamma(1) + \Delta DIC(2)\times\gamma(2) + \cdots + \Delta DIC(x)\times\gamma(x)}. \quad (21)$$

where $\Delta TA(j)$ and $\Delta DIC(j)$ represent changes due to the j^{th} biogeochemical reaction (e.g., $\Delta TA(j) = -2$ and $\Delta DIC(j) = 0$ for sulfide oxidation; Table 1), and $\gamma(j)$ represents the molar numbers of the j^{th} reaction as listed in Table 1. Accordingly, the contributions of the specific reaction ($\Delta TA(j)\times\gamma(j)$ and $\Delta DIC(j)\times\gamma(j)$) to the overall biogeochemical reaction terms (ΔTA_i and ΔDIC_i) can be quantified as follows:

$$TA\%(j) = \frac{\Delta TA(j)\times\gamma(j)}{\Delta TA_i}\times 100\% \quad (22)$$

$$DIC\%(j) = \frac{\Delta DIC(j)\times\gamma(j)}{\Delta DIC_i}\times 100\% \quad (23)$$

Table 1 only includes several major biogeochemical processes that affect TA and DIC. For simplicity, we choose five major reactions and assume Redfield reaction stoichiometry for a detailed examination of the MAE data (Table 3). There are numerous combinations from the five reactions that can result in the same β value, and three possible cases are listed ($\beta = 1.1$; Table 3). It is evident that the contribution of the specific reaction can vary significantly. For instance, in cases I and II, sulfide oxidation is not considered, and the system is slightly autotrophic, with primary production slightly exceeding aerobic remineralization. The relative contributions of primary production and aerobic remineralization to the overall

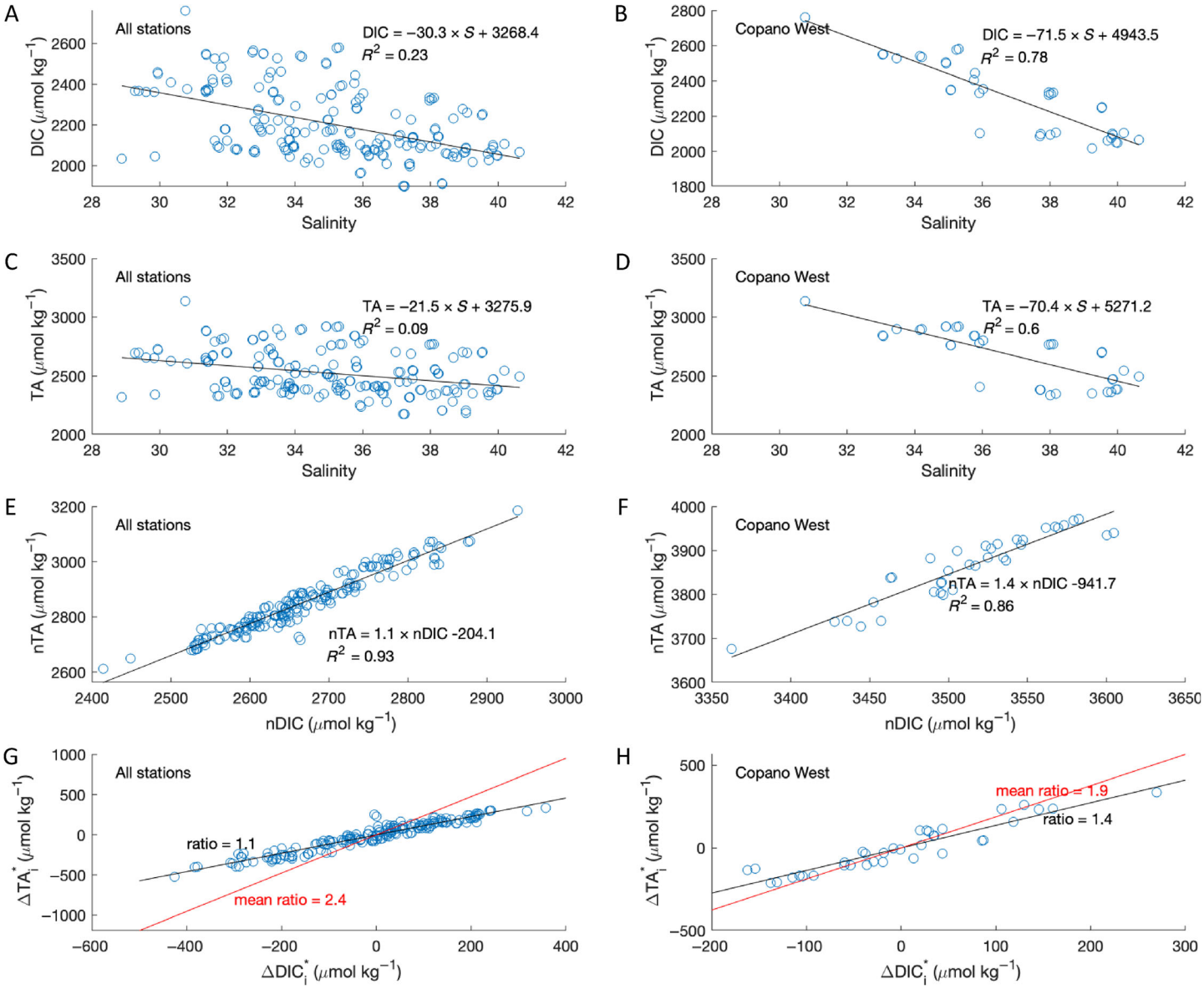

Fig. 2. DIC–salinity, TA–salinity, nTA–nDIC, and $\Delta TA_i^* - \Delta DIC_i^*$ relationships from all stations in the MAE (**A**,**C**,**E**,**G**) and Copano West station only (**B**,**D**, **F**,**H**). $S_{ref} = 20$. The linear regression slopes for nTA–nDIC are 1.1 for all stations (**E**) and 1.4 for Copano West (**F**). The ratios of 1.1 (**G**) and 1.4 (**H**) are also indicated by the black lines in the $\Delta TA_i^* - \Delta DIC_i^*$ plots, and the red lines indicate the mean ratios of all data in each analysis.

changes in TA and DIC vary, and in case II, carbonate dissolution plays a relatively important role in TA variation (TA% [4] = 92% and TA% ranges from −188% to 196%). When sulfide oxidation is included, as in case III, its contribution to TA change (TA% [5] = −1176%) can be significant compared to the other reactions (TA% ranges from −2400% to 2500%). The examples provided in Table 3 are all theoretically possible and demonstrate that relying solely on β value will not be sufficient to quantitatively discern the metabolic processes driving the variations in TA and DIC. Therefore, the subjective assignment of processes could introduce biases in the interpretation.

Only positive ΔTA_i and positive ΔDIC_i are considered in the above discussion to reach a ratio value of β. However, negative ΔTA_i and negative ΔDIC_i can also lead to the same β. Including these possibilities would further complicate the discussions. Furthermore, using the $\Delta TA_i^*/\Delta DIC_i^*$ method can also cause problems. Due to the theoretical basis of the least squares regression method, both positive and negative differences (i.e., observation above and below the regression line) must coexist (Fig. 1A,B). Thus, the data located in the first quartile of the $\Delta TA_i^* - \Delta DIC_i^*$ plot (positive ΔTA_i^* and ΔDIC_i^*; Figs. 1D, 2G,H) does not necessary indicate addition of both

Table 3. Possible contributions of five reactions to the slope ($\beta = 1.1$) of the nTA–nDIC relationship. γ, TA%, and DIC% are defined in Eqs. 21–23.

Process		R1—primary production (nitrate)	R2—aerobic remineralization (nitrate)	R3—CO_2 dissolution	R4—carbonate dissolution	R5—sulfide oxidation
I	γ	25	24	125.5	5	0
	TA%	1574	−1511	0	37	0
	DIC%	−10,796	10,364	511	20	0
II	γ	25	24	203.3	100	0
	TA%	196	−188	0	92	0
	DIC%	−1343	1290	103	51	0
III	γ	25	24	21.5	100	100
	TA%	2500	−2400	0	1176	−1176
	DIC%	−17,147	16,461	139	647	0

TA and DIC, and vice versa for the data located in the third quartile. The addition or consumption of TA or DIC should be estimated relative to the conservative mixing values after evaporation correction, which requires endmember values and evaporation factor, instead of the linear regression of observations.

Other limitations also exist when applying this ratiometric method. Assuming organic matter with the Redfield composition and deriving reaction stoichiometry can be problematic. In marine systems, the C : N : P ratio in organic matter can vary significantly, leading to variations in the reaction stoichiometry. Many studies have observed spatial and temporal variations in the Redfield ratio (e.g., Frigstad et al. 2011; Moreno and Martiny 2018; Singh et al. 2013; Talarmin et al. 2016). These studies suggest that using a universal C:N:P ratio for organic matter in interpreting the nTA–nDIC relationship and $\Delta TA_i^*/\Delta DIC_i^*$ may also pose issues.

In summary, we recommend that the TA and DIC data should not be solely relied upon for interpreting the metabolic processes in the coastal ocean, because the simple deduction method could lead to erroneous interpretations. Instead, it is important to consider other parameters simultaneously for a comprehensive analysis. For example, chlorophyll levels can serve as a direct indicator of primary production, nitrate enrichment and depletion (N*) can support the occurrence of nitrification and denitrification, respectively, and dissolved oxygen levels can provide information on whether it is aerobic or anerobic process. By incorporating multiple parameters, a more robust understanding of the metabolic processes can be achieved using the inorganic carbon measurements.

References

Brewer, P. G., and J. C. Goldman. 1976. Alkalinity changes generated by phytoplankton growth 1. Limnol. Oceanogr. **21**: 108–117. doi:10.4319/lo.1976.21.1.0108

Cabral, A., T. Dittmar, M. Call, J. Scholten, C. E. de Rezende, N. Asp, M. Gledhill, M. Seidel, and I. R. Santos. 2021. Carbon and alkalinity outwelling across the groundwater-creek-shelf continuum off Amazonian mangroves. Limnol. Oceanogr. Lett. **6**: 369–378. doi:10.1002/lol2.10210

Cai, W.-J., Y. Wang, J. Krest, and W. Moore. 2003. The geochemistry of dissolved inorganic carbon in a surficial groundwater aquifer in North Inlet, South Carolina, and the carbon fluxes to the coastal ocean. Geochim. Cosmochim. Acta **67**: 631–639. doi:10.1016/S0016-7037(02)01167-5

Chen, G.-T., and F. J. Millero. 1979. Gradual increase of oceanic CO_2. Nature **277**: 205–206. doi:10.1038/277205a0

Courtney, T. A., T. Cyronak, A. J. Griffin, and A. J. Andersson. 2021. Implications of salinity normalization of seawater total alkalinity in coral reef metabolism studies. PLoS One **16**: e0261210. doi:10.1371/journal.pone.0261210

Dias, L. M., X. Hu, and H. Yin. 2022. A biogeochemical alkalinity sink in a shallow, semiarid estuary of the northwestern Gulf of Mexico. Aquat. Geochem. **29**: 49-71. doi:10.1007/s10498-022-09410-z

Dickson, A. G. 1981. An exact definition of total alkalinity and a procedure for the estimation of alkalinity and total inorganic carbon from titration data. Deep Sea Res. A Oceanogr. Res. Pap. **28**: 609–623. doi:10.1016/0198-0149(81)90121-7

Dickson, A. G., C. L. Sabine, and J. R. Christian. 2007. Guide to best practices for ocean CO2 measurements. North Pacific Marine Science Organization. doi:10.25607/OBP-1342

Frigstad, H., T. Andersen, D. O. Hessen, L.-J. Naustvoll, T. M. Johnsen, and R. G. Bellerby. 2011. Seasonal variation in marine C:N:P stoichiometry: Can the composition of seston explain stable Redfield ratios? Biogeosciences **8**: 2917–2933. doi:10.5194/bg-8-2917-2011

Friis, K., A. Körtzinger, and D. W. Wallace. 2003. The salinity normalization of marine inorganic carbon chemistry data. Geophys. Res. Lett. **30**: 1085. doi:10.1029/2002GL015898

Goldman, J. C., and P. G. Brewer. 1980. Effect of nitrogen source and growth rate on phytoplankton-mediated changes in alkalinity. Limnol. Oceanogr. **25**: 352–357. doi:10.4319/lo.1980.25.2.0352

Gran, G. 1952. Determination of the equivalence point in potentiometric titrations. Part II. Analyst **77**: 661–671. doi:10.1039/an9527700661

Hunt, C. W., J. E. Salisbury, and D. Vandemark. 2022. Controls on buffering and coastal acidification in a temperate estuary. Limnol. Oceanogr. **67**: 1328–1342. doi:10.1002/lno.12085

Liu, Y., J. J. Jiao, W. Liang, I. R. Santos, X. Kuang, and C. E. Robinson. 2021. Inorganic carbon and alkalinity biogeochemistry and fluxes in an intertidal beach aquifer: Implications for ocean acidification. J. Hydrol. **595**: 126036. doi:10.1016/j.jhydrol.2021.126036

McCutcheon, M. R, and X. Hu. 2021. Carbonate chemistry in mission aransas estuary from May 2014 to Feb 2017 and Dec 2018 to Feb 2020. Biological and chemical oceanography data management office (BCO-DMO). doi:10.26008/1912/bco-dmo.835227.1

Middelburg, J. J., K. Soetaert, and M. Hagens. 2020. Ocean alkalinity, buffering and biogeochemical processes. Rev. Geophys. **58**: e2019RG000681. doi:10.1029/2019RG000681

Millero, F. J., K. Lee, and M. Roche. 1998. Distribution of alkalinity in the surface waters of the major oceans. Mar. Chem. **60**: 111–130. doi:10.1016/S0304-4203(97)00084-4

Mooney, R. F., and J. W. McClelland. 2012. Watershed export events and ecosystem responses in the Mission–Aransas National Estuarine Research Reserve, South Texas. Estuar. Coast. **35**: 1468–1485. doi:10.1007/s12237-012-9537-4

Moreno, A. R., and A. C. Martiny. 2018. Ecological stoichiometry of ocean plankton. Ann. Rev. Mar. Sci. **10**: 43–69. doi:10.1146/annurev-marine-121916-063126

Orr, J. C., J.-M. Epitalon, A. G. Dickson, and J.-P. Gattuso. 2018. Routine uncertainty propagation for the marine carbon dioxide system. Mar. Chem. **207**: 84–107. doi:10.1016/j.marchem.2018.10.006

Peng, T.-H., R. Wanninkhof, J. L. Bullister, R. A. Feely, and T. Takahashi. 1998. Quantification of decadal anthropogenic CO_2 uptake in the ocean based on dissolved inorganic carbon measurements. Nature **396**: 560–563. doi:10.1038/25103

Singh, A., M. Lomas, and N. Bates. 2013. Revisiting N2 fixation in the North Atlantic Ocean: Significance of deviations from the Redfield ratio, atmospheric deposition and climate variability. Deep-Sea Res. II Top. Stud. Oceanogr. **93**: 148–158. doi:10.1016/j.dsr2.2013.04.008

Su, J., and others. 2020. Chesapeake Bay acidification buffered by spatially decoupled carbonate mineral cycling. Nat. Geosci. **13**: 441–447. doi:10.1038/s41561-020-0584-3

Szymczycha, B., M. E. Böttcher, M. Diak, K. Koziorowska-Makuch, K. Kuliński, P. Makuch, C. M. E. von Ahn, and A. Winogradow. 2023. The benthic-pelagic coupling affects the surface water carbonate system above groundwater-charged coastal sediments. Front. Mar. Sci. **10**: 1218245. doi:10.3389/fmars.2023.1218245

Talarmin, A., M. W. Lomas, Y. Bozec, N. Savoye, H. Frigstad, D. M. Karl, and A. C. Martiny. 2016. Seasonal and long-term changes in elemental concentrations and ratios of marine particulate organic matter. Global Biogeochem. Cycl. **30**: 1699–1711. doi:10.1002/2016GB005409

Van Dam, B. R., and others. 2021. Calcification-driven CO_2 emissions exceed "Blue Carbon" sequestration in a carbonate seagrass meadow. Sci. Adv. **7**: eabj1372. doi:10.1126/sciadv.abj1372

Wolf-Gladrow, D. A., R. E. Zeebe, C. Klaas, A. Körtzinger, and A. G. Dickson. 2007. Total alkalinity: The explicit conservative expression and its application to biogeochemical processes. Mar. Chem. **106**: 287–300. doi:10.1016/j.marchem.2007.01.006

Xiong, T., H. Li, Y. Yue, Y. Hu, W.-D. Zhai, L. Xue, N. Jiao, and Y. Zhang. 2023. Legacy effects of late macroalgal blooms on dissolved inorganic carbon pool through alkalinity enhancement in Coastal Ocean. Environ. Sci. Technol. **57**: 2186–2196. doi:10.1021/acs.est.2c09261

Yang, B., and R. H. Byrne. 2023. Sub-annual and inter-annual variations of total alkalinity in the northeastern Gulf of Mexico. Mar. Chem. **250**: 104195. doi:10.1016/j.marchem.2022.104195

Yin, H., X. Hu, and L. M. Dias. 2023. Sulfate enrichment in estuaries of the northwestern Gulf of Mexico: The potential effect of sulfide oxidation on carbonate chemistry under a changing climate. Limnol. Oceanogr. Lett. **8**: 742–750. doi:10.1002/lol2.10335

Acknowledgments

This study was supported by the National Science Foundation (OCE #1654232). H.Y. and X.H. also acknowledge partial support from both the National Science Foundation (OCE #2319434) and Louisiana State University. The support from Louisiana State University was provided through a subaward funded by the National Aeronautics and Space Administration under grant #80NSSC23K0126.

Submitted 29 January 2024
Accepted 01 March 2024

Associate editor: Mike DeGrandpre